Available online at www.sciencedirect.com
ScienceDirect
Scripta Materialia 62 (2010) 333–336
Scripta MATERIALIA
www.elsevier.com/locate/scriptamat

A maximum in ductility and fracture toughness in nanostructured Cu/Cr multilayer films

J.Y. Zhang,[a] G. Liu,[a,*] X. Zhang,[a] G.J. Zhang,[a] J. Sun[a,*] and E. Ma[a,b]

[a]*State Key Laboratory for Mechanical Behavior of Materials, Xi'an Jiaotong University, Xi'an 710049, China*
[b]*Department of Materials Science and Engineering, Johns Hopkins University, Baltimore, MD 21218, USA*

Received 21 August 2009; revised 21 October 2009; accepted 22 October 2009
Available online 25 October 2009

In Cu/Cr multilayers with modulation period (λ) ranging from 10 to 250 nm, maxima are observed for both tensile ductility and fracture at a critical $\lambda \sim 50$ nm, different from the monotonic λ dependence known for monolithic films. This unusual behavior is explained, via quantitative assessments based on a micromechanical model, by considering the competing thickness effects on the size of the microcracks initiated in the Cr layers and on the role of the ductile Cu layer in blocking crack propagation.

Keywords: Nanostructured multilayers; Ductility; Toughness; Size effect

Nanostructured multilayer films (NMFs) are not only scientifically interesting but also useful for many technological applications [1–5]. At room temperature, NMFs with nanoscale modulation periods (denoted as λ) can withstand stresses as high as 1/2–1/3 of the theoretical strength [6–8]. In both face-centered cubic (fcc)/body-centered cubic (bcc) type (e.g. Cu/Cr [6], Cu/Nb [6] and Al/Nb [9]) and fcc/fcc type (e.g. Cu/Ag [10] and Cu/Ni [10]) NMFs the strength increases monotonically with decreasing λ. The trend for the accompanying tensile ductility of the NMFs is the opposite: generally it decreases with decreasing λ [2].

In this paper, we report that in some NMFs composed of alternating soft/hard layers, the toughness and tensile ductility do not exhibit a monotonic λ dependence. Instead, there exists a critical λ at which the ductility (or toughness) reaches a peak. We illustrate the underlying mechanism, and demonstrate the ductilization/constraint effect of the soft layers on the hard (more brittle) layers.

Cu/Cr NMFs deposited on compliant polymer substrates are chosen as the model materials here (this configuration is similar to that of flexible electronics [11,12] and helps to suppress strain localization [13,14]). A macroscopic strain (ε_C) corresponding to a critical degree of microcracking (measured in situ using an electrical resistance change method, ERCM [15]), in lieu of the rupture strain or elongation, is used to characterize the ductility. The fracture toughness of the Cu/Cr NMFs is derived using a micromechanical model.

Polyimide-supported Cu/Cr NMFs (total thickness ~500 nm) with equal individual layer thickness h_M but different λ ($\lambda = 2h_M$) of 10, 25, 50, 62.5, 100 and 250 nm were synthesized by means of direct current (DC) magnetron sputtering at room temperature. X-ray diffraction revealed a strong ⟨1 1 1⟩ out-of-plane texture for the Cu layers and a weak ⟨1 1 0⟩ out-of-plane texture for Cr layers, while the in-plane orientations are random. Cross-sectional views of the NMFs from the transmission electron microscopy (TEM) observations are displayed in Figure 1, and show columnar grains in the Cu layers and ultrafine nanocrystals in the Cr layers. The average grain sizes of both Cu and Cr scale with layer thickness. It can be seen that there are bright fringes along the interface between the Cu layer and Cr layer (e.g. in Fig. 1b). Further high-resolution (HR) TEM examinations reveal that these fringes are a very thin (~2 nm) intermixing layer, as typically shown in Figure 1c. The disordered regions of intermixing layer arise from intermixing between Cu and Cr driven by the surface energy during the non-equilibrium deposition process, which is similar to previous reports in the binary immiscible metallic multilayers such as Ag/Ni [15] and Ag/Nb [16]. For comparison, single-layer monolithic Cr thin films with thicknesses (h) in the 25–200 nm range were also prepared on the polyimide substrate. No columnar porosities have been detected

* Corresponding author; E-mail: lgsammer@mail.xjtu.edu.cn, junsun@mail.xjtu.edu.cn

1359-6462/$ - see front matter © 2009 Acta Materialia Inc. Published by Elsevier Ltd. All rights reserved.
doi:10.1016/j.scriptamat.2009.10.030

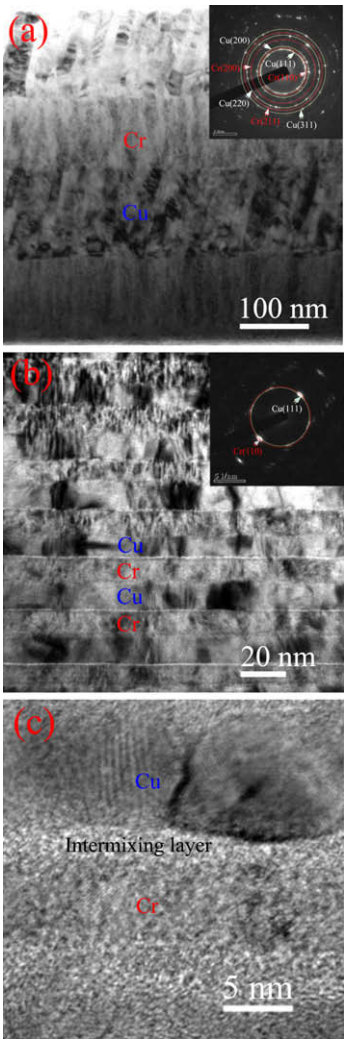

Figure 1. Bright-field cross-sectional TEM micrograph showing the microstructure of the Cu/Cr NMFs with (a) $\lambda = 250$ nm and (b) $\lambda = 25$ nm. Insert shows the corresponding selected area diffraction patterns (SADPs). (c) HRTEM image typically showing a very thin intermixing layer (~2 nm) formed at the Cu/Cr interface.

in both the multilayer and the single-layer films. After annealing at 150 °C for 2 h, residual stress of the films has been measured by X-ray diffraction using the "sin2ψ method" [17,18]. The residual stress in the single-layer Cr films is determined to be about 200 ± 50 MPa, varying less with thickness. Similarly, the residual stress in the multilayer films is also insensitive to the modulation periods, having a value of 250 ± 150 MPa. Uniaxial tensile testing was performed using a Micro-Force Test System (MTS® Tytron 250) at a constant strain rate of $1 \times 10^{-4}\ s^{-1}$ at room temperature. The dog-bone shaped samples had a total length of 65 mm, and a gauge section of 30 mm in length and 4 mm in width. The displacement was recorded via a HR laser detecting system [19,20]. In order to analyze the failure mechanism, tested Cu/Cr NMMFs were cross-sectioned and characterized using a FEI dual-beam focused ion beam/scanning electron microscope (FIB/SEM).

Figure 2a shows the dependence of ε_C on h_M or h. The single-layer films (shown here for Cr; Cu behaves the same way) are known to exhibit a monotonic decrease of ε_C as h is reduced [19]. Interestingly, over this h_M range the ε_C of the NMFs increases first, followed by a peak at a critical $h_M^{cri} \sim 25$ nm (or $\lambda^{cri} \sim 50$ nm). Below h_M^{cri}, ε_C decreases with reducing h_M (λ), similar to the behavior of single-layer films, while above h_M^{cri}, a smaller h_M leads to higher ε_C (ε_C is doubled when h_M is reduced from 125 to 25 nm). Compared with the $h = 25$ nm monolithic Cr, the ε_C of the NMF is a factor of 5 higher. As mentioned above, the residual stress in the single-layer Cr film and multilayer films is insensitive to the film thickness and the modulation period, respectively, and the two kinds of films have similar residual stress. This indicates that the present experimental results are not predominantly related to the residual stress. It is the introduction of the soft Cu layers that is responsible for the improvement of the ductility.

Figure 2b–d show the cross-sectional SEM images of the tested samples with $\lambda = 250$, 50 and 25 nm, respectively. Microcracks are seen to initiate within, and run across, the Cr layer, which is the more brittle of the two constituent materials (especially since it tends to incorporate some oxygen during deposition). Further propagation of the microcracks is arrested by the more ductile Cu layers (Fig. 2b). Whether the microcracks can be stopped depends on two factors. The first is the intensity of stress–strain fields (ISFs) ahead of the microcrack tip. ISF scales with $\sqrt{h_M}$ [21] as the size of the crack is approximately h_M. This would lead to the expectation that a smaller h_M is favorable for suppressed

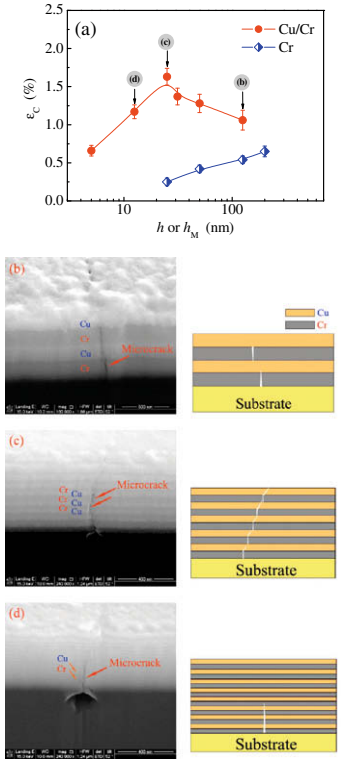

Figure 2. (a) Dependence of ε_C on h_M for the Cu/Cr NMFs and on h for the single-layer Cr films. Lines are visual guides. The (b) $h_M = 125$ nm, (c) $h_M = 25$ nm and (d) $h_M = 12.5$ nm samples after tests are displayed in the corresponding panels, respectively, with SEM cross-sectional images of microcracks and schematics of their behavior.

crack growth and improved ductility. The other factor is the shielding on microcrack propagation by the plastic deformation (dislocation) activities in Cu, which become rather limited when the h_M is too small. This renders very thin Cu less effective in improving ductility. The two competing effects lead to the peak in the λ dependence and the maximum in ductility observed in Figure 2a.

Above h_M^{cri}, plastic deformation in the Cu layers is not a problem and the ISF is the controlling factor. Reducing h_M would then promote crack suppression and improve ε_C. Indeed, comparing Figure 2b and c, shorter and multiple isolated cracks are observed in thinner Cr layers. Only at $h_M = 125$ nm can the microcrack in the Cr layer overcome the Cu shielding effect and penetrate across the entire NMF. Below h_M^{cri}, the very thin Cu layers themselves become more and more brittle as they lose the ability to accommodate dislocation activities, weakening the shielding effect of the Cu layers. The microcracks in the Cr layers, although small, can now break loose to cause failure (Fig. 2d). As a result, the NMF ductility behavior reverses to decrease with h_M (Fig. 2a).

The propagation of microcracks can be analyzed in the framework of fracture mechanics. The fracture toughness (K_{IC}) of the films is generally given by [22]:

$$K_{IC} = \sqrt{\frac{E\xi}{1-\nu^2}}, \tag{1}$$

where E is the Young's modulus of the metal films, ν is the Poisson's ratio ($\sim$1/3) and ξ is the steady-state energy release rate [23]:

$$\xi = \frac{\pi\sigma^2 h_T}{2E}(1-\nu^2)g(\alpha,\beta), \tag{2}$$

where σ is the tensile stress of the films at the critical point of ε_C, which can be determined from the stress–strain curve of the films, h_T is the total film thickness, and $g(\alpha,\beta)$ is a dimensionless quantity that can be calculated from the elastic mismatch between the film and substrate, with α and β being the two Dundurs' parameters [24]. For our case, $\alpha \cong 0.95$ and $\beta = \alpha/4$. Using experimental data together with Eqs. (1) and (2), the calculated K_{IC} as a function of h_M is shown in Figure 3a. The λ-dependent K_{IC} behaves similarly to ε_C, which also has a maximum at $h_M = 25$ nm.

The K_{IC} behavior in fact compares well quantitatively with predictions obtained from a micromechanical fracture model [25] in laminates consisting of alternating ductile and brittle layers (see Fig. 3b); this model was constructed based on the dislocation blunting of crack tips and dislocations piling up at an interface and sending a back-stress to the crack tip, hindering further dislocation emission. At a given load level, the equilibrium number (n) of dislocations is [25]:

$$n = \frac{4\pi(1-\nu)}{\ln\left(\tilde{h}/\tilde{r}\right)}\left(\frac{\tilde{K}_{app}\sqrt{\tilde{h}}}{A\sqrt{2\pi}}\sin\phi\cos\frac{\phi}{2} - \tilde{\gamma}\right), \tag{3}$$

where ϕ is the angle that the slip plane inclines from the interface (chosen as 45°); A is a factor slightly greater

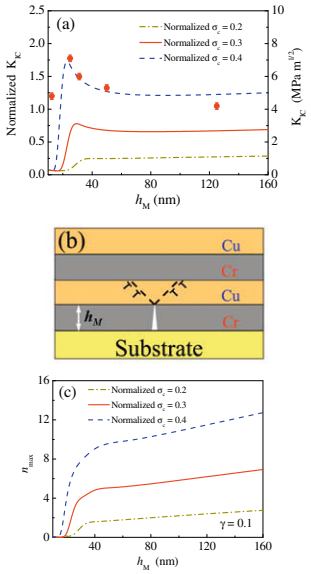

Figure 3. (a) Dependence of K_{IC} on h_M (dots and right y-axis) for the Cu/Cr NMFs. Calculated normalized K_{IC} (dashed lines) are also included for comparison. (b) Sketch of the micromechanical fracture model. (c) Model predicted $n_{\max}$ at different normalized cohesive strengths ($\tilde{\sigma}_c$) as a function of h_M.

than unity; $\tilde{r} \approx 2.7r_0/b$ with r_0 being the effective core radius and b the Burgers vector of the dislocation in the ductile material; $\tilde{K}_{app}$, $\tilde{h}$ and $\tilde{\gamma}$ are the normalized values of the far-field mode I stress intensity K_{app} (=1.12 $\sigma_{app}\sqrt{\pi h_M}$ [21]), the maximum distance $h_\phi = h_M/\sin\phi$ that the leading dislocation can travel and the surface energy γ, respectively.

$$\tilde{K}_{app} = \frac{K_{app}}{\mu\sqrt{b}}, \tilde{h} = \frac{h_\phi}{b}, \tilde{\gamma} = \frac{\gamma}{\mu b}, \tag{4}$$

where μ is the shear modulus of the Cu layers. The tensile stress at the blunted crack tip ($\tilde{\sigma}_{tip} = \sigma_{tip}/\mu$) is related to n and $\tilde{K}_{app}$ as [25]:

$$\tilde{\sigma}_{tip}\sqrt{n} = 2\sqrt{\frac{2}{\pi}}\tilde{K}_{app}\left(1 - \frac{3\left(\sin\phi\cos\frac{\phi}{2}\right)^2}{\ln(\tilde{h}/\tilde{r})}\right) + \frac{12A}{\sqrt{\tilde{h}}\ln(\tilde{h}/\tilde{r})}\tilde{\gamma}\sin\phi\cos\frac{\phi}{2}. \tag{5}$$

Upon increasing the applied load, further dislocation emission competes with the cleavage at the blunted crack tip. When the microcrack tip tensile stress $\tilde{\sigma}_{tip}$ reaches the normalized cohesive strength of the material, $\tilde{\sigma}_c$ (=σ_c/μ), fracture occurs in the ductile Cu layer and the microcrack will propagate to form a channel crack. According to Hsia et al. [25], the fracture mode of various confined layered metals is likely to be cleavage because the movement of dislocations is greatly restricted. The far-field applied stress intensity under this condition is then the fracture toughness of the layered films, i.e. $\tilde{K}_{IC} = \tilde{K}_{app}|_{\tilde{\sigma}_{tip}=\tilde{\sigma}_c}$. Based on this criterion, the maximum number of dislocations emitted from the microcrack tip prior to fracture ($n_{\max}$) and then the $\tilde{K}_{IC}$ can be

obtained from Eqs. (3) and (5). Calculated results[1] of $\tilde{K}_{IC}$ vs. h_M shown in Figure 3a also reveals a maximum value at $h_M \sim 25$ nm. In particular, the calculations at $\tilde{\sigma}_c = 0.4$ fit well with the measurements.

The predicted $n_{\max}$, Figure 3c, lends support to the explanation given above. Below h_M^{cri}, it can be seen that $n_{\max}$ sharply decreases when h_M is reduced down to less than about h_M^{cri}, quantitatively demonstrating that the Cu layer will lose much of its plastic deformation capability when a few dislocations are emitted. Conversely, with appropriate selection of h_M at or slightly above h_M^{cri}, a brittle material can be toughened via the multilayer scheme, Figure 2a, without sacrificing much of the strength.

This work was supported by the National Basic Research Program of China (Grant No. 2004CB619303 & 2010CB631003) and the National Natural Science Foundation of China (50971097).

[1] A. Misra, J.P. Hirth, R.G. Hoagland, Acta Mater. 53 (2005) 4817.
[2] H.B. Huang, F. Spaepen, Acta Mater. 48 (2000) 3261.
[3] M.A. Phillips, B.M. Clemens, W.D. Nix, Acta Mater. 51 (2003) 3157.
[4] J. Wang, P.M. Anderson, Acta Mater. 53 (2005) 5089.
[5] M.J. Demkowicz, R.G. Hoagland, J.P. Hirth, Phys. Rev. Lett. 100 (2008) 136102.
[6] A. Misra, M. Verdie, Y.C. Lu, H. Kung, T.E. Mitchell, M. Nastasi, J.D. Embury, Scripta Mater. 39 (1998) 555.
[7] A. Misra, R.G. Hoagland, J. Mater. Res. 20 (2005) 2046.
[8] J.D. Embury, J.P. Hirth, Acta Metall. Mater. 42 (1994) 2051.
[9] E.G. Fu, N. Li, A. Misra, R.G. Hoagland, H. Wang, X. Zhang, Mater. Sci. Eng. A493 (2008) 283.
[10] J. McKeown, A. Misra, H. Kung, R.G. Hoagland, M. Nastasi, Scripta Mater 46 (2002) 593.
[11] S.R. Forrest, Nature (London) 428 (2004) 911.
[12] J. Hwang, A. Wan, A. Kahn, Mater. Sci. Eng. R 64 (2009) 1.
[13] T. Li, Z.Y. Huang, Z.C. Xi, S.P. Lacour, S. Wagner, Z. Suo, Mech. Mater. 37 (2005) 261.
[14] Y. Xiang, T. Li, Z. Suo, J. Vlassak, Appl. Phys. Lett. 87 (2005) 161910.
[15] B.M. Clemens, W.D. Nix, V. Ramaswamy, J. Appl. Phys. 87 (2000) 2816.
[16] W.S. Lai, M.J. Yang, Appl. Phys. Lett. 90 (2007) 181917.
[17] Ph. Goudeau, K.F. Badawi, A. Naudon, G. Gladyszewski, Appl. Phys. Lett. 62 (1993) 246.
[18] B. Girault, P. Villain, E. Le Bourhis, P. Goudeau, P.O. Renault, Surf. Coat. Tech. 201 (2006) 4372.
[19] R.M. Niu, G. Liu, C. Wang, G. Zhang, X.D. Ding, J. Sun, Appl. Phys. Lett. 90 (2007) 161907.
[20] D.Y.W. Yu, F. Spaepen, J. Appl. Phys. 95 (2004) 2991.
[21] R.W. Hertzberg, Deformation and Fracture Mechanics of Engineering Materials, John Wiley, New York, 1989.
[22] L.B. Freund, S. Suresh, Thin Film Materials: Stress, Defect Formation, and Surface Evolution, Cambridge University Press, Cambridge, 2003.
[23] J.L. Beuth Jr., Int. J. Solids Struct. 29 (1992) 1657.
[24] J. Dundurs, D.B. Bogy, J. Appl. Mech. 36 (1969) 650.
[25] K.J. Hsia, Z. Suo, W. Yang, J. Mech. Phys. Solids 42 (1994) 877.

[1] Value of the parameters for calculations are: $\mu = 48.3$ GPa, $b = 0.256$ nm, $r_0 = 1.725$ nm. $\tilde{\sigma}_c$ is taken in the range from 0.2 to 0.4, applicable to ductile metals such as Cu, Al and Au.